EVM Calculation for Broadband Modulated Signals[*]

Michael D. McKinley[1], Kate A. Remley[1], Maciej Myslinski[2], J. Stevenson Kenney[3], Dominique Schreurs[2], Bart Nauwelaers[2]

[1]Electromagnetics Division, National Institute of Standards and Technology
mckinm, remley@boulder.nist.gov,
[2]ESAT-TELEMIC, Katholieke Universiteit Leuven, Belgium
Maciej.Myslinski, Dominique.Schreurs, Bart.Nauwealears@esat.kuleuven.ac.be
[3]Georgia Institute of Technology, jskenney@ece.gatech.edu

Abstract: We present a normalization that facilitates calculation of error vector magnitude (EVM) from measurements. We derive the definition of EVM for a common industry standard from a more basic equation. We compare EVM for various modulation types for a given average symbol power under simple distortion conditions.

Keywords: Digital Modulation; Error Vector Magnitude; Vector Signal Analyzer; Wireless Telecommunications.

I. Introduction

Error vector magnitude (EVM) is a common figure of merit for assessing the quality of digitally modulated telecommunication signals. EVM expresses the difference between the expected complex voltage value of a demodulated symbol and the value of the actual received symbol. While another common figure of merit, bit error rate, gives a "go," "no-go" level of system characterization, EVM can be more useful to the microwave engineer because it contains information about both amplitude and phase errors in the signal [1], [2]. This additional information can allow a more complete picture of the channel distortion and is more closely related to the physics of the system.

Because of the potential for mixing of in-band frequency components, EVM is often used to characterize signals that use broadband schemes for transmitting large amounts of data at relatively high speeds. The most common of these schemes at 5 GHz is known as orthogonal frequency-division multiplexing (OFDM), as specified by the IEEE 802.11a[TM]-1999 standard [2], [3]. OFDM is used in wireless local-area networks (WLANs), in the Dedicated Short-Range Communication (DSRC) systems for tracking and observing loads in commercial vehicles [4], and in the recently opened public-safety band at 4.9 GHz.

The IEEE 802.11a[TM]-1999 standard specifies use of several different OFDM modulation types (i.e., binary phase-shift keying (BPSK), quadrature phase-shift keying (QPSK), 16-symbol quadrature amplitude modulation (16QAM), 64-symbol quadrature amplitude modulation (64QAM), etc.) that may be used in adjacent bursts. Even within one burst more than one modulation format may be used since the four pilot subcarriers are always transmitted using BPSK. This motivates the use of normalization, to calculate EVM easily and to enable direct comparison of EVM for a given average power level per symbol between modulation types. Such normalization is implicit in the IEEE 802.11a[TM]-1999 standard and is the focus of this paper.

We first briefly introduce a common representation of demodulated symbols for the digital modulation types used in the IEEE 802.11a[TM]-1999 standard. Following this, we derive a normalization that lets us find EVM by comparing an ideal symbol value to one that is measured. This direct calculation of EVM means that, on a normalized plot, the magnitude of the error vector for each symbol equals the symbol's EVM. The normalization also aids the comparison of

---

EVM for various modulation types for a given average symbol power. Finally, we compare EVM for the different modulation types used in the IEEE 802.11a™-1999 standard.

II. Normalization to Enable Direct EVM Calculation and Comparison

EVM measurements are often performed on vector signal analyzers (VSAs), real-time analyzers or other instruments that capture a time record and internally perform a Fast Fourier Transform (FFT) to enable frequency-domain analysis. Calculation of EVM is often accomplished through software internal to these instruments. Signals are downconverted and demodulated before EVM calculations are made. As discussed above, to calculate and compare EVM efficiently for different modulation types, some normalization is typically carried out.

A. Constellation Diagrams and EVM

To aid in the visualizing of demodulated signals, constellation diagrams are often used to represent digital bits in terms of symbols. In a sense, constellation diagrams are the bridge between digital and analog representations of a data stream. A constellation diagram is a plot of symbols where each symbol represents one or more bits (depending on the modulation type)—the digital aspect. It is also a plot where each symbol is represented by a unique magnitude and phase—the analog aspect.

Figure 1 shows three constellation diagrams for 16QAM, which has 16 symbols that modulate the RF carrier in both magnitude and phase. In each case, I and Q represent the in-phase (0° relative phase) and quadrature (90° relative phase) values of each symbol. This gives each symbol a resulting magnitude and phase. Figure 1(a) represents a measured set of symbols. The V_I and V_Q axes give, respectively, the measured in-phase and quadrature (90° relative phase) voltage levels for a complex voltage representation. Scattered dots on this diagram represent the effect of small errors in the measured symbols. Figure 1(b) represents the ideal constellation described below. The units of the in-phase and quadrature axes are dimensionless integers and are represented by C_I and C_Q, respectively.

To efficiently calculate EVM, the diagrams in Figs. 1(a) and 1(b) are scaled to form the normalized (dimensionless) constellation diagram in Fig. 1(c). The in-phase (S_I) and quadrature (S_Q) axes are similar to the real and imaginary axes used in complex voltage representations. We derive a scaling for these constellations in this section.

To enable the normalization, we assume a uniform distribution of the transmitted symbols onto the constellation. This means that the transmitted symbols have an equal probability of visiting each location on the constellation and that the number of symbols transmitted is a multiple of the number of unique symbols in a constellation. We also assume that before normalization occurs the receiver has derotated the received symbols so that they are aligned in the constellation. Systematic rotation of symbols can occur, for example, when there is a difference between the sampling frequency (typically set by the center frequency) and that of a given subcarrier. In this case, the rotation is greatest on the outermost subcarriers and enlarges with each subsequent OFDM symbol received. Due to the commonality of the problem, all OFDM receivers have derotation operations built into them.

Ideal Constellation. Constellation diagrams that show the ideal placement of symbols for a given modulation type are often represented by symbols at integer levels. We saw this in Fig. 1(b), where the constellation diagram for 16QAM was shown.

Furthermore, the number of levels along either an in-phase or quadrature axis for an ideal constellation is

$$n = \sqrt{N} \quad . \tag{1}$$

For example, since $N = 16$ for 16QAM, there are four symbol levels ($n = 4$) for both the in-phase and quadrature axes. The integer coordinates of the ideal constellation points for each symbol are

$$C_{\text{ideal},pq} = C_{\text{I,ideal},pq} + jC_{\text{Q,ideal},pq} = (2p - 1 - n) + j(2q - 1 - n) \quad , \tag{2}$$

where the integers p and q satisfy $1 \le p \le n$, $1 \le q \le n$, and the integer n is defined in (1). From (2), we can obtain what we refer to here as the "ideal constellation diagram," Fig. 1(b), for any of the common digital modulation types.
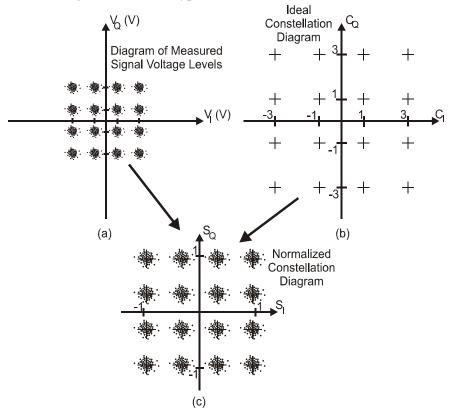

Figure 1: Graphs of (a) measured symbols, (b) the ideal constellation diagram, and (c) a normalized space that facilitates calculation of EVM.

Normalized Constellation. Figure 2 again shows the normalized constellation diagram representation from Fig. 1(c). Our normalization is derived such that the mean-square amplitude of all possible symbols in the constellation is one, as discussed below. Figure 2 also shows the error vector for one measured symbol. In this special case with only one measured symbol, the magnitude of this small vector equals the EVM. If there were more symbols acquired than just this one, the EVM would equal the sum of the magnitudes of the error vectors for all of the measured symbols divided by the total number of measured symbols.

Thus, when symbols have been normalized, EVM is defined as the root-mean-square (RMS) value of the difference between a collection of measured symbols and ideal symbols (also RMS quantities). These differences are averaged over a given, typically large, number of symbols and are often shown as a percent of the average power per symbol of the constellation.

As given in (2) of [5], EVM can be expressed mathematically as

$$EVM_{\text{RMS}} = \left[\frac{\dfrac{1}{N}\displaystyle\sum_{r=1}^{N} |\, S_{\text{ideal},r} - S_{\text{meas},r}\,|^2}{\dfrac{1}{N}\displaystyle\sum_{r=1}^{N} |\, S_{\text{ideal},r}\,|^2} \right]^{\frac{1}{2}}, \tag{3}$$

where $S_{\text{meas},r}$ is the normalized r^{th} symbol in a stream of measured symbols, $S_{\text{ideal},r}$ is the ideal normalized constellation point for the rth symbol, and N is the number of unique symbols in the constellation.[1]
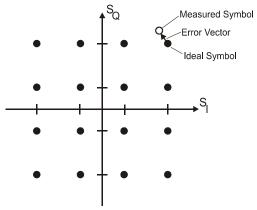

Figure 2: Normalized constellation diagram for 16QAM [1].

B. Normalizations of the measured and ideal representations

To find EVM, we must compare the ideal symbol values from the ideal constellation diagram to the arbitrary voltage values that we measure. One way to enable this comparison is to normalize both the measured and ideal symbols, as illustrated in Fig. 1. We describe this procedure below.

Measured Case. For the measured case, one method for accomplishing this normalization is to divide the power in each symbol, $P_{V,\text{symbol}}$, by the average symbol power calculated over all symbols in the constellation, to obtain $P_{S,\text{symbol}}$:

$$P_{S,\text{symbol}} = \frac{P_{V,\text{symbol}}}{P_V / T}, \tag{4}$$

where P_V, the total power of a measured constellation having T symbols, is

$$P_V = \sum_{r=1}^{T} \left[\left(V_{\text{I,meas},r} \right)^2 + \left(V_{\text{Q,meas},r} \right)^2 \right] \text{ (W)}, \tag{5}$$

where $V_{\text{I or Q,meas},r}$ is the RMS voltage level of the in-phase and quadrature components of the measured symbols and T is typically $\gg N$.

---

[1] Thus, $N = 16$ for the 16QAM case. For the measured case, averaging is typically carried out. Thus, N should be replaced with T = total number of symbols measured. Typically, $T \gg N$.

From (4), we see that $P_{S,symbol}$, is dimensionless. The average of all $P_{S,symbol}$'s in the normalized constellation will be equal to one. For example, the normalized constellation for 16QAM is given in Fig. 3.

To calculate EVM, we must represent this normalization in terms of voltage. We identify a normalization factor $|A_{meas}|$ from (4) as

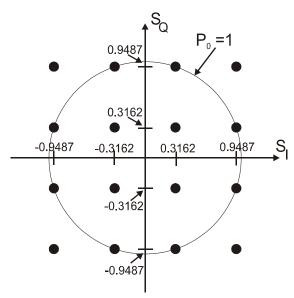$$|A_{meas}| = \sqrt{\frac{1}{P_V/T}} \qquad . \qquad (6)$$

Figure 3: Normalized constellation diagram.

Ideal Case. For the ideal case, we carry out the normalization in an integer space rather than a voltage space. However, a similar procedure can be used for the integer space if we use N instead of T where N is the number of unique symbols in a constellation (e.g., 4 for QPSK or 16 for 16QAM). In this case, P_C does not represent the total power in a constellation as does P_V, but is rather the sum of the squares of the amplitudes of all symbols:

$$P_C = \sum_{p=1}^{n} \left[\sum_{q=1}^{n} \left(C_{I,ideal,pq}^{2} + C_{Q,ideal,pq}^{2} \right) \right] \qquad . \qquad (7)$$

Here, $C_{I,ideal,pq}$ and $C_{Q,ideal,pq}$ are, respectively, the real (in-phase) and imaginary (quadrature) integer values corresponding to each symbol, and n is defined in (1). Note that for the ideal, integer-based constellation diagram (Fig. 1(b)), P_C can also be found by substituting the values in (2) for C_I and C_Q:

$$P_C = \sum_{p=1}^{n} \left[\sum_{q=1}^{n} \left((2p-1-n)^2 + (2q-1-n)^2 \right) \right] \cdot \qquad (8)$$

Similar to (6), the normalization scaling factor for ideal symbols, $|A_{ideal}|$, is written as

$$|A_{\text{ideal}}| = \sqrt{\frac{1}{P_{\text{C}}/N}} \qquad . \qquad (9)$$

Normalized EVM. From (6) and (9), EVM can be represented as

$$EVM_{\text{RMS}} = \left[\frac{\frac{1}{T}\sum_{r=1}^{T}\left(\left\|(V_{\text{I,meas},r})\cdot|A_{\text{meas}}| - (C_{\text{I,ideal},r})\cdot|A_{\text{ideal}}|\right\|^2 + \left\|(V_{\text{Q,meas},r})\cdot|A_{\text{meas}}| - (C_{\text{Q,ideal},r})\cdot|A_{\text{ideal}}|\right\|^2\right)}{P_{\text{S,avg}}} \right]^{\frac{1}{2}}, \quad (10)$$

where

$$P_{\text{S,avg}} = \frac{1}{N}\sum_{p=1}^{n}\left[\sum_{q=1}^{n}\left((2p-1-n)^2|A_{\text{ideal}}|^2 + (2q-1-n)^2|A_{ideal}|^2\right)\right] . \qquad (11)$$

In (11), $P_{\text{S,avg}}$ is the normalized mean-square amplitude of the symbols in the constellation. It is always equal to one, and is the same as P_0 in [1]. $V_{\text{I or Q,meas},r}$ and $C_{\text{I or Q,ideal},r}$ are the unnormalized voltages and integer values, respectively, for the rth symbol for the measured and ideal in-phase and quadrature components. The quantities A_{meas} and A_{ideal} refer, respectively, to the normalization factors in (6) and (9) calculated for the measured and ideal constellations. The limit T encompasses all measured symbols and satisfies the relation $T \gg N$.

C. EVM and the IEEE 802.11a[TM]-1999 standard

From the representation of (10), we can easily derive the expression for EVM in the IEEE 802.11a[TM]-1999 standard. We first identify the normalized voltages in terms of I and Q to get

$$EVM_{\text{RMS}} = \left[\frac{\frac{1}{T}\sum_{r=1}^{T}\left(|I_r - I_{0,r}|^2 + |Q_r - Q_{0,r}|^2\right)}{P_0} \right]^{\frac{1}{2}} , \qquad (12)$$

where $I_r = (V_{\text{I,meas},r})\cdot|A_{\text{meas}}|$, $\quad Q_r = (V_{\text{Q,meas},r})\cdot|A_{\text{meas}}|$, $\quad I_{0,r} = (C_{\text{I,ideal},r})\cdot|A_{\text{ideal}}|$, $\quad$ and $Q_{0,r} = (C_{\text{Q,ideal},r})\cdot|A_{\text{ideal}}|$.

The IEEE 802.11a[TM]-1999 standard includes some of the specifics of the multiplexing types: the subcarriers (52 total), the length of the packets (i.e., the number of symbols in a packet), L_{P}, and the number of frames received, N_{f}. This gives us the equation given in [1]:

$$EVM_{\text{RMS}} = \frac{\sum_{i=1}^{N_{\text{f}}}\left[\frac{\sum_{j=1}^{L_{\text{P}}}\left\{\sum_{k=1}^{52}\left[|I(i,j,k) - I_0(i,j,k)|^2 + |Q(i,j,k) - Q_0(i,j,k)|^2\right]\right\}}{52\cdot L_{\text{P}}\cdot P_0}\right]^{\frac{1}{2}}}{N_{\text{f}}} . \qquad (13)$$

With the normalization derived above applied in (13), we are able to compare EVM across subcarriers, packets and frames for bursts with different modulation types as long as the average

power per symbol and the center frequency of the signal are consistent. The ability to directly compare EVM for different modulation types is important since the IEEE standard specifies use of BPSK modulation for the four pilot subcarriers, while the 48 remaining data subcarriers may utilize a different modulation scheme. By including all 52 subcarriers, (13) is able to include, for example, errors on the composite signal due to frequency-response effects across its wide bandwidth or frequency-dependent distortion effects due to nonlinear amplification.

III. EVM for Different Modulation Types in Different Environments

We used two measurement set-ups to test the effects of simple channel distortion on EVM across different modulation types. We generated modulated signals in the IEEE 802.11a[TM]-1999 standard at 5 GHz using a vector signal generator (VSG). The 5 GHz signals were downconverted externally and sent to our vector signal analyzer. One test set-up was designed to represent a low-distortion, best-case scenario for our instrumentation. In this case, we fed the output of our VSG directly to the frequency converter through a cable. This set-up is the same as that shown in Fig. 4 but with the tuner and splitter/combiner replaced with one cable.

For the second test, we intentionally introduced distortion to increase EVM. We split the signal from the VSG into two branches, as shown in Fig. 4. We fed one branch through a cable to an impedance tuner that introduced some phase shift and distortion of the modulated signal, while the other branch was fed through a cable. The two branches were then recombined and down-converted to the frequency range of our VSA.
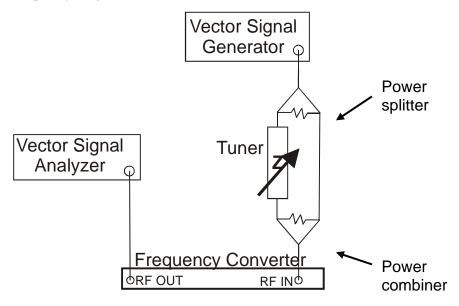

Figure 4: Higher-distortion test set-up for measuring EVM.

We measured EVM using the VSA for all of the modulation types used in the IEEE 802.11a[TM]-1999 standard. We used a commercial package to calculate the EVM for the composite signal, as in (13). The specification for EVM in the data sheet of this commercial package is <1 %. Our EVM for the low-distortion case was within this range, as shown in Fig. 5(a). For each measurement of the low-distortion case, we received an average symbol power of ~1.77 μW (9.41 $\pm$ 0.04 mV$_{rms}$ across 50 Ω) with all 48 data subcarriers set to the same modulation format.

Results for the higher-distortion set-up are shown in Fig. 5(b). For each measurement in this set-up, we measured an average symbol power of ~28.5 nW (1.194 $\pm$ 0.006 mV$_{rms}$ across 50 Ω) with all 48 data subcarriers set to the same modulation format. The relatively low increase in

overall EVM for the higher-distortion case can be attributed to a cyclic prefix that is included in the IEEE 802.11a[TM]-1999 standard to minimize the effects of multipath distortion. The cyclic prefix is obtained by copying the rear part of a burst and attaching it to the front. By allowing any carry-over energy due to multipath effects or intersymbol interference from a previous burst to fall into the cyclic prefix and not into the main signal, the effects of these types of interference on EVM are minimized.
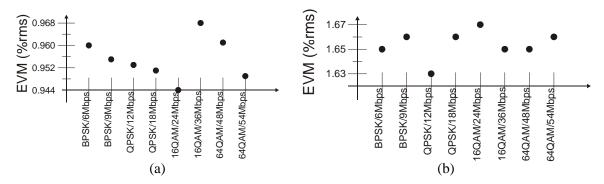

Figure 5: EVM for the modulation types used in the IEEE 802.11a[TM]-1999 standard for (a) a low-distortion case and (b) a higher-distortion case utilizing a two-path channel and a tuner.

Our measurements demonstrate that the normalization defined by (10) does enable direct comparison of EVM for the different modulation types for a given average symbol power. While EVM did change between the two setups, little change occurred between the various modulation types. The EVM values in Fig. 5 for both the low- and high-distortion cases varied by less than 0.05 %. On a scale showing 0-1 % EVM or 0-2 % EVM for the low and high EVM cases, respectively, the plotted points resemble a flat line.

IV. Discussion and Conclusions

We derived a normalization for measured symbols and constellation diagrams that enables ready calculation of EVM. This involved multiplying the in-phase and quadrature voltages for each measured or ideal symbol in the constellation by a factor that yields a mean-square symbol amplitude with a value of one. We showed the equivalence of our normalized representation of EVM and the EVM in the IEEE 802.11a[TM]-1999 standard. This demonstration went from a simple mathematical representation to one that takes frames, packet length and all 52 subcarriers into account. We compared measurements of EVM for different modulation types in the IEEE 802.11a[TM]-1999 standard for simple low- and high-distortion scenarios.

References:
[1] IEEE Standard for Wireless LAN Medium Access Control (MAC) and Physical Layer (PHY) Specifications: High-Speed Physical Layer in the 5 GHz Band, IEEE Standard 802.11a[TM]-1999.
[2] IEEE Standard for Wireless LAN Medium Access Control (MAC) and Physical Layer (PHY) Specifications: Higher-Speed Physical Layer Extension in the 2.4 GHz Band, IEEE Standard 802.11b-1999.
[3] This standard is identified solely for completeness of description, but such identification does not constitute an endorsement by the National Institute of Standards and Technology. Other products may work as well or better.
[4] http://www.leearmstrong.com/DSRC/DSRCHomeset.htm
[5] S. Forestier, P. Bouysse, R. Quere, A. Mallet, J.-M. Nebus, and L. Lapierre, "Joint optimization of the power-added efficiency and the error-vector measurement of 20-GHz pHEMT amplifier through a new dynamic bias-control method," *IEEE Trans. Microwave Theory and Tech*, vol. 52, no.4, pp. 1132-1140, Apr. 2004.